J|A|C|S ARTICLES

Published on Web 11/03/2009

Photoconversion of the Fluorescent Protein EosFP: A Hybrid Potential Simulation Study Reveals Intersystem Crossings

Mickaël Lelimousin,[†,‡,§] Virgile Adam,[||] G. Ulrich Nienhaus,[⊥,#] Dominique Bourgeois,[†,‡,§,||] and Martin J. Field*[,†,‡,§]

CNRS, UMR5075, Institut de Biologie Structurale Jean-Pierre Ebel, 41 rue Jules Horowitz, 38027 Grenoble Cedex 1, France, CEA, DSV, Grenoble F-38027, France, Université Joseph Fourier, Grenoble, F-38000, France, European Synchrotron Radiation Facility, 6 Rue Jules Horowitz, BP 220, 38043 Grenoble Cedex, France, Institute of Applied Physics and Center for Functional Nanostructures, Karlsruhe Institute of Technology, 76131 Karlsruhe, Germany, and Department of Physics, University of Illinois at Urbana−Champaign, 1110 West Green Street, Urbana, Illinois 61801

Received June 30, 2009; E-mail: martin.field@ibs.fr

Abstract: Fluorescent proteins undergoing green to red photoconversion have proved to be essential tools in cell biology, notably in superlocalization nanoscopy. However, the exact mechanism governing photoconversion, which overall involves irreversible cleavage of the protein backbone and elongation of the chromophore π-conjugation, remains unclear. In this paper we present a theoretical investigation of the photoconversion reaction in the fluorescent protein EosFP, using excited-state hybrid quantum chemical and molecular mechanical potentials, in conjunction with reaction-path-finding techniques. Our results reveal a mechanism in which the hydroxybenzylidene moiety of the chromophore remains protonated and there is an excited state proton transfer from His62 to Phe61 that promotes peptide bond cleavage. Excitation of the neutral green form of EosFP to the first singlet excited state is followed by two intersystem crossing events, first to a triplet state and then back to the ground state singlet surface. From there, a number of rearrangements occur in the ground state and lead to the red form. Analyses of the structures and energies of the intermediates along the reaction path enable us to identify the critical role of the chromophore environment in promoting photoinduced backbone cleavage. Possible ways in which photoconvertible fluorescent proteins can be engineered to facilitate photoconversion are considered.

Introduction

During the past 15 years, fluorescent proteins (FPs) have become indispensable tools in cell biology, as their use as markers has revolutionized understanding of cellular processes.[1,2] Some of these proteins can change their photophysical properties on exposure to light. Such modifications in photoactivatable fluorescent proteins include reversible switching between a fluorescent "on" state and a nonfluorescent "off" state and irreversible photoconversion between a green- and a red-emitting state.[3] The structures of the green and red forms of several photoconvertible fluorescent proteins (PCFPs) have been determined by X-ray crystallography, including EosFP,[4] KikGR,[5] Kaede,[6] and IrisFP.[7] Because of the utility of these proteins for investigating movements in live cells[3] or designing super-resolution imaging schemes based on the photoactivated localization microscopy approach,[8] considerable work has gone into optimizing PCFPs. This led to the recent development of the monomeric variants Dendra2,[9] mEos2,[10] and mKikGR,[11] which proved to be more suitable for designing functional fusion constructs.

A conserved triad of residues, His62-Tyr63-Gly64, characterizes the chromophore of PCFPs. As for all members of the GFP family, the chromophore is enclosed in the center of an 11-

[†] CNRS, Institut de Biologie Structurale Jean-Pierre Ebel.
[‡] CEA, Institut de Biologie Structurale Jean-Pierre Ebel.
[§] Université Joseph Fourier, Institut de Biologie Structurale Jean-Pierre Ebel.
[||] European Synchrotron Radiation Facility.
[⊥] Karlsruhe Institute of Technology.
[#] University of Illinois at Urbana−Champaign.

(1) Shaner, N. C.; Patterson, G. H.; Davidson, M. W. *J. Cell Sci.* **2007**, *120*, 4247–4260.
(2) Nienhaus, G. U. *Angew. Chem., Int. Ed.* **2008**, *47*, 8992–8994.
(3) Wiedenmann, J.; Nienhaus, G. U. *Exp. Rev. Proteomics* **2006**, *3*, 361–734.
(4) Nienhaus, K.; Nienhaus, G. U.; Wiedenmann, J.; Nar, H. *Proc. Natl. Acad. Sci. U.S.A.* **2005**, *102*, 9156–9159.
(5) Tsutsui, H.; Karasawa, S.; Shimizu, H.; Nukina, N.; Miyawaki, A. *EMBO Rep.* **2005**, *6*, 233–238.
(6) Hayashi, I.; Mizuno, H.; Tong, K. I.; Furuta, T.; Tanaka, F.; Yoshimura, M.; Miyawaki, A.; Ikura, M. *J. Mol. Biol.* **2007**, *372*, 918–926.
(7) Adam, V.; Lelimousin, M.; Boehme, S.; Desfonds, G.; Nienhaus, K.; Field, M. J.; Wiedenmann, J.; McSweeney, S.; Nienhaus, G. U.; Bourgeois, D. *Proc. Natl. Acad. Sci. U.S.A.* **2008**, *105*, 18343–18348.
(8) Betzig, E.; Patterson, G. H.; Sougrat, R.; Lindwasser, O. W.; Olenych, S.; Bonifacino, J. S.; Davidson, M. W.; Lippincott-Schwartz, J.; Hess, H. F. *Science* **2006**, *313*, 1642–1645.
(9) Gurskaya, N. G.; Verkhusha, V. V.; Shcheglov, A. S.; Staroverov, D. B.; Chepurnykh, T. V.; Fradkov, A. F.; Lukyanov, S.; Lukyanov, K. A. *Nat. Biotechnol.* **2006**, *24*, 461–465.
(10) McKinney, S. A.; Murphy, C. S.; Hazelwood, K. L.; Davidson, M. W.; Looger, L. L. *Nat. Methods* **2009**, *6*, 131–133.
(11) Habuchi, S.; Tsutsui, H.; Kochaniak, A. B.; Miyawaki, A.; van Oijen, A. M. *PLoS One* **2008**, *3*, e3944.

 10.1021/ja905380y CCC: $40.75

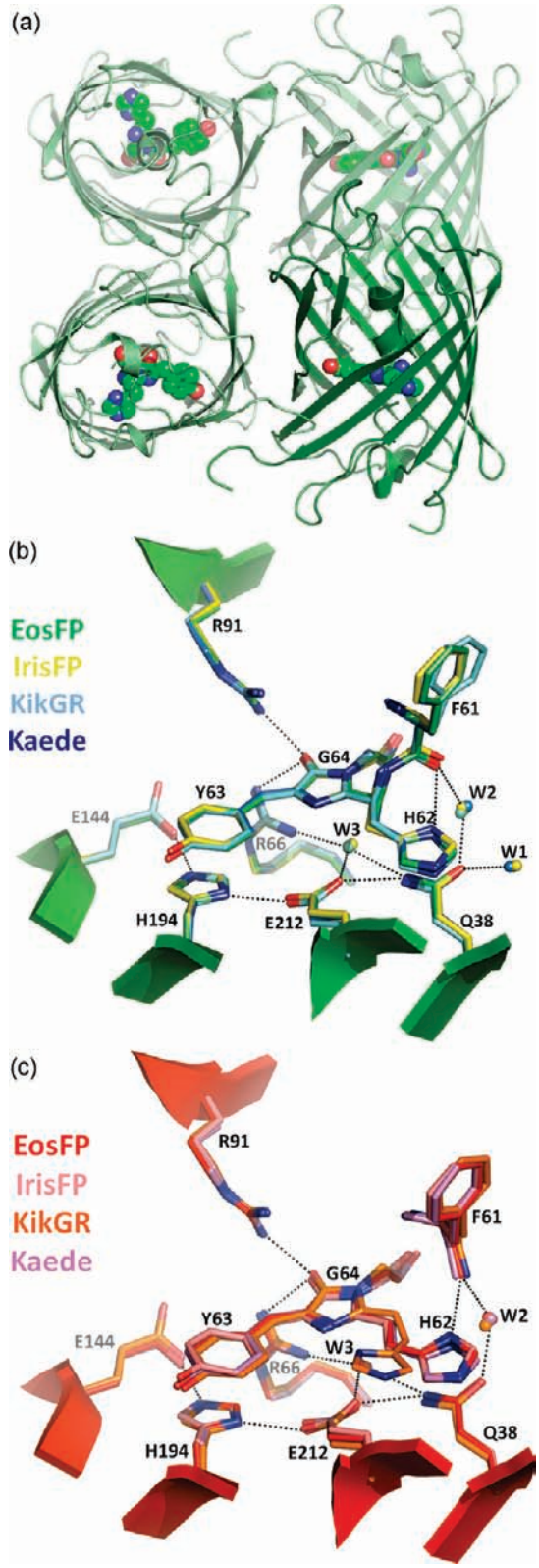

Figure 1. (a) Tetrameric structure of wt-EosFP. Chromophores are shown as van der Waals spheres. (b) Superposition of the chromophore and surrounding residues in the green forms of EosFP, IrisFP, KikGR, and Kaede (hydrogen bonds are indicated by dotted lines). (c) Superposition of the chromophore and surrounding residues in the red forms of EosFP, IrisFP, KikGR and Kaede (hydrogen bonds are indicated by dotted lines).

stranded β-barrel structure (Figure 1a), where it is rigidly held by an environmental network of hydrogen bonds and van der Waals interactions (Figure 1b). The green form of PCFPs arises via autocatalytic maturation in the dark, yielding a 4-(*p*-hydroxybenzylidene)-5-imidazolinone π-conjugated system. Illumination with UV light causes cleavage of the peptide bond between the amide nitrogen of residue 61 and the α-carbon of His62, formation of a double bond on the His62 side chain, and extension of the conjugated system to a 2-[(1*E*)-2-(5-imidazolyl)-ethenyl]-4-(*p*-hydroxybenzylidene)-5-imidazolinone moiety,[4,12] leading to the red-emitting form. Despite these changes, the three-dimensional structure of the protein is almost completely preserved in the red form (Figure 1c). However, a water molecule (W1) that is present in the structures of green EosFP, IrisFP, and Kaede is not observed in the red forms. This water molecule is absent from both the green and red forms of KikGR, which is characterized by an additional isomerization of the His62 side chain.

The basic (anionic) form of PCFP chromophores absorbs around 500 nm, and the acidic (neutral) form around 390 nm. Although it has been reported that very intense illumination at 488 nm converts Dendra2,[9] possibly in the anionic form of the chromophore, it is generally accepted that photoconversion only occurs in the neutral (phenolic) form.[3,11,13−15] The reaction is irreversible: neither keeping the protein in the dark nor under illumination with visible light at any wavelength can restore the green state.[13] Measurements of rate constants for the photoconversion of PCFPs revealed much slower kinetics than for other photoinduced reactions such as photoisomerization.[11,16] As a consequence, the quantum yield of photoconversion in PCFPs is low ($\sim 10^{-3}-10^{-4}$).[5,7,11,13] Photoconversion can be abolished by substitution of His62 with any other amino acid,[12,14] thereby asserting this residue's critical role, and by various other mutations in the chromophore's environment.[12,17]

To date, the exact mechanism of green-to-red photoconversion in PCFPs remains unknown, although several hypotheses have been proposed. Using NMR structures of Kaede, Mizuno et al. suggested initially that the imidazole of His62 could become biprotonated and that this would facilitate backbone cleavage via β-elimination.[12] On the basis of the X-ray crystallographic structures of EosFP in both its green and red states, Nienhaus et al. proposed an excited state proton transfer (ESPT) from the hydroxyl group of Tyr63 to the N_ε of His62, followed by a β-elimination step in which Glu212 acts as a proton acceptor.[4] Finally, Hayashi et al. proposed a water-assisted mechanism to explain the loss of the water molecule W1 in the red form of Kaede.[6]

A detailed experimental investigation of photoconversion is difficult because of its low quantum yield and irreversibility. In contrast, molecular simulation can provide important insights into the photoconversion mechanism. Especially appropriate tools in this endeavor are hybrid quantum chemical/molecular mechanical (QC/MM) potentials because they are well adapted

(12) Mizuno, H.; Mal, T. K.; Tong, K. I.; Ando, R.; Furuta, T.; Ikura, M.; Miyawaki, A. *Mol. Cell* **2003**, *12*, 1051–1058.
(13) Ando, R.; Hama, H.; Yamamoto-Hino, M.; Mizuno, H.; Miyawaki, A. *Proc. Natl. Acad. Sci. U.S.A.* **2002**, *99*, 12651–12656.
(14) Wiedenmann, J.; Ivanchenko, S.; Oswald, F.; Schmitt, F.; Rocker, C.; Salih, A.; Spindler, K. D.; Nienhaus, G. U. *Proc. Natl. Acad. Sci. U.S.A.* **2004**, *101*, 15905–15910.
(15) Adam, V.; Nienhaus, K.; Bourgeois, D.; Nienhaus, G. U. *Biochemistry* **2009**, *48*, 4905–4915.
(16) Dittrich, P. S.; Schafer, S. P.; Schwille, P. *Biophys. J.* **2005**, *89*, 3446–3455.
(17) Nienhaus, G. U.; Nienhaus, K.; Holzle, A.; Ivanchenko, S.; Renzi, F.; Oswald, F.; Wolff, M.; Schmitt, F.; Rocker, C.; Vallone, B.; Weidemann, W.; Heilker, R.; Nar, H.; Wiedenmann, J. *Photochem. Photobiol.* **2006**, *82*, 351–358.

for studying phenomena that require a quantum mechanical description but which occur in large systems. Most reported QC/MM studies of photochemical reactions in proteins concern ultrafast events.[18] Examples include photoisomerization of chromophores in rhodopsins,[19] photoactive yellow protein,[20] and other fluorescent proteins.[21] In this paper, we investigate theoretically the mechanism of the green-to-red photoconversion in EosFP, which is a typical representative of the PCFP family. By employing hybrid QC/MM potentials in conjunction with reaction-path-finding techniques, we propose that two intersystem crossing (ISC) events to the triplet state T_1 and back to the ground state S_0 are critical for forming the red-emitting state. Structural determinants of the EosFP chromophore pocket for efficient photoconversion are also investigated, and general conclusions about PCFPs are drawn.

Methods

All simulations were performed with the fDynamo library.[22] The starting structures for the simulations were those of the tetramers determined by X-ray crystallography for the green (PDB id: 1ZUX) and red (PDB id: 2BTJ) forms of EosFP.[4] The positions of the hydrogen atoms were determined after the protonation states of the residues in the protein had been estimated at a pH of 7.0, using standard Poisson−Boltzmann calculations.[23] All residues were determined to have their expected protonation, with the exception of His194, for which the pK_a calculation and examination of the X-ray crystallographic structures suggested a biprotonation at pH 7.0 (Figure 1b and c). The resulting protein structures were geometry-optimized in vacuum using the OPLS-AA force field.[24] The optimized tetrameric structures were then solvated and optimized in a cubic water box of the appropriate size, employing the TIP3P MM water model.[25] Counterions were added to ensure charge neutrality of the overall system. The final systems comprised approximately 43,100 atoms.

QC/MM simulations were performed starting from the two prepared MM systems. Unless explicitly stated in the text, the QC region consisted of 65 atoms and contained the chromophore and the side chains of two amino acid residues: Glu212, which has been proposed to play an essential role in photoconversion, and His194, which is involved in π-stacking with the hydroxybenzylidene moiety (Figure 1b and c). Atoms in the MM region were treated with the OPLS-AA force field and those in the QC region with either the AM1[26] or the PDDG-PM3[27] semiempirical methods. The results obtained with the two potentials are qualitatively and, in most cases, quantitatively similar, so that we only show the PDDG-PM3 results in the main paper. The AM1 results are given as Supporting Information.

To calculate the energy and atomic forces of the system in both ground and excited states, a standard configuration interaction (CI) method was incorporated into the fDynamo library. The CI method itself permits calculations with a number of possible configuration sets, either all configurations within a given active space (full CI) or a mixture of single and double excitations (CIS, CID, and CISD) from a closed-shell singlet reference state. Gradients of the energy are calculated with the Z-matrix technique.[28,29] Our tests showed that a ten-electron/nine-orbital or [10,9]-CISD approximation gave the best compromise between accuracy and computational time. Sample results for our systems are given in Table S1 (note: all table and figure numbers preceded by "S" are located in Supporting Information). To simplify the discussion, we refer to the [10,9]-CISD(PDDG-PM3)/OPLS and [10,9]-CISD(AM1)/OPLS hybrid potentials as the PDDG and AM1 potentials, respectively.

To assess the accuracy of the semiempirical methods, we also performed time-dependent density functional theory calculations using the ORCA quantum chemical program.[30] Experience showed that the results were more sensitive to the functional that was employed than the basis set. Hence, the calculations reported here are with the BP86 and B3LYP functionals and the SVP (split valence with polarization) basis set.[31]

To investigate the photoconversion reaction, we employed the nudged elastic band (NEB) method[32] to determine minimum energy paths (MEPs) between various, selected reactant and product structures. Although MEPs do not directly give time-scale or thermodynamic information, they can provide useful information about possible mechanisms, including the identity of intermediates, the order in which events occur, and estimates of barrier heights.

All NEB calculations were done using the A monomer of the prepared systems. To reduce the computational expense of the optimization, only the ~840 atoms within 12 Å of the C_α atom of His62 were allowed to move. The remaining atoms were fixed, although their interactions with the mobile atoms were taken into account. The complete photoconversion pathway could not be determined by a single NEB calculation between green and red forms because of the complexity and the multiplicity of the reaction steps and the different electronic states upon which the reaction occurs. Reaction paths were determined between geometry-optimized start and end structures, on either the ground or excited states, and using at least 11 structures along the pathway. Whenever suggested by intersystem crossings, results were refined by recalculating parts of the reaction path between specific intermediates at the appropriate electronic state. In all energy profiles, the labels of intermediate structures are placed above the energy point if the path was minimized in an excited state and below if it was minimized in the ground state. The zero of energy is taken to be the energy of the neutral green form in its ground state. Its vertical excitation to S_1 is estimated to be ~345 kJ/mol for both the QC/MM potentials that were used.

Results and Discussion

Previous Mechanistic Proposals. Scheme 1 provides a summary of the steps putatively involved in the previously proposed photoconversion mechanism of EosFP: an ESPT from the hydroxybenzylidene group of the chromophore to the N_ε of His62, followed by a β-elimination reaction in which Glu212 acts as a proton acceptor.[4] The (arbitrary) notation that we use for the various intermediate structures throughout this work is also provided in Scheme 1. Our initial simulations were performed to test the mechanism of Scheme 1 by calculating NEB pathways on the excited state singlet (S_1) for the first step and on the ground state singlet (S_0) surface for all following

(18) Virshup, A. M.; Punwong, C.; Pogorelov, T. V.; Lindquist, B. A.; Ko, C.; Martinez, T. J. *J. Phys. Chem. B* **2009**, *113*, 3280–3291.
(19) Hayashi, S.; Tajkhorshid, E.; Schulten, K. *Biophys. J.* **2009**, *96*, 403–416.
(20) Groenhof, G.; Schafer, L. V.; Boggio-Pasqua, M.; Grubmuller, H.; Robb, M. A. *J. Am. Chem. Soc.* **2008**, *130*, 3250–3251.
(21) Schafer, L. V.; Groenhof, G.; Boggio-Pasqua, M.; Robb, M. A.; Grubmuller, H. *PLoS Comput. Biol.* **2008**, *4*, e1000034.
(22) Field, M. J.; Albe, M.; Bret, C.; Proust-De Martin, F.; Thomas, A. *J. Comput. Chem.* **2000**, *21*, 1088–1100.
(23) Antosiewicz, J.; Mccammon, J. A.; Gilson, M. K. *J. Mol. Biol.* **1994**, *238*, 415–436.
(24) Jorgensen, W. L.; Maxwell, D. S.; TiradoRives, J. *J. Am. Chem. Soc.* **1996**, *118*, 11225–11236.
(25) Jorgensen, W. L.; Chandrasekhar, J.; Madura, J. D.; Impey, R. W.; Klein, M. L. *J. Chem. Phys.* **1983**, *79*, 926–935.
(26) Dewar, M. J. S.; Zoebisch, E. G.; Healy, E. F.; Stewart, J. J. P. *J. Am. Chem. Soc.* **1985**, *107*, 3902–3909.
(27) Repasky, M. P.; Chandrasekhar, J.; Jorgensen, W. L. *J. Comput. Chem.* **2002**, *23*, 1601–1622.
(28) Handy, N. C.; Schaefer, H. F. *J. Chem. Phys.* **1984**, *81*, 5031–5033.
(29) Patchkovskii, S.; Thiel, W. *Theor. Chem. Acc.* **1997**, *98*, 1–4.
(30) Neese, F. ORCA Quantum Chemistry Program. http://www.thch.uni-bonn.de/tc/orca/.
(31) Koch, W.; Holthausen, M. C. *A Chemist's Guide to Density Functional Theory*; Wiley-VCH: New York, NY, 2000.
(32) Galvan, I. F.; Field, M. J. *J. Comput. Chem.* **2008**, *29*, 139–143.

Scheme 1. Hypothetic Photoconversion Mechanism Inspired from Nienhaus et al.,[4] with Intermediate Structures Derived from Simulation[a]

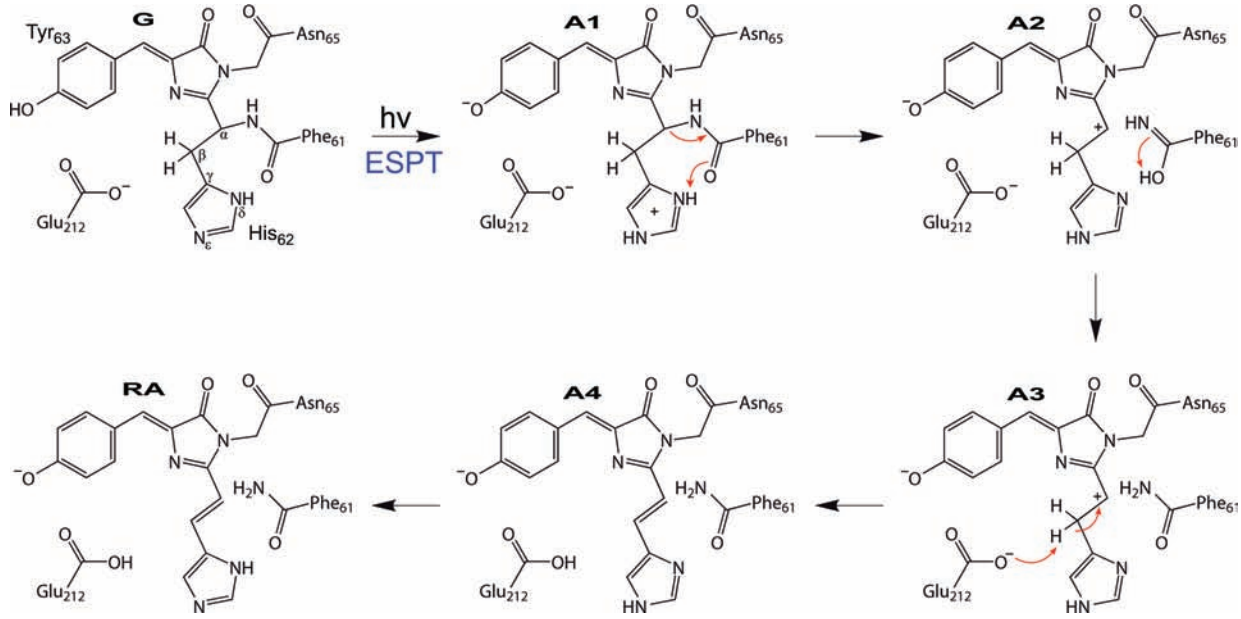

[a] Arrows show the main reaction steps in red (color assigned to the ground state S_0 throughout the paper).

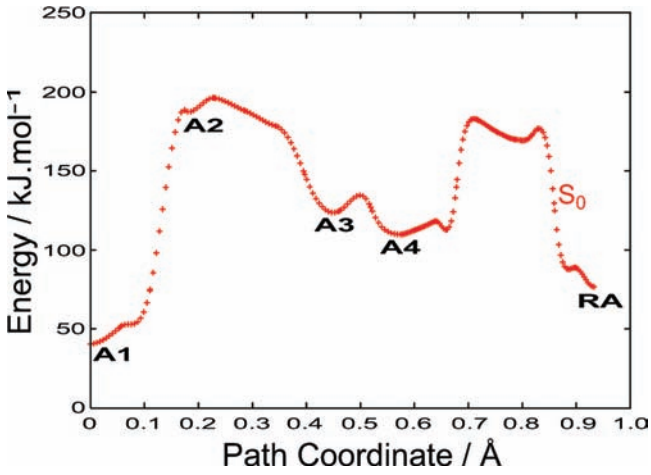

Figure 2. Energy profile of optimized NEB paths from A1 to A4 and from A4 to RA in the ground state S_0 calculated with a PDDG/OPLS hybrid potential.

steps. The energy profiles obtained for these latter are shown in Figures 2 and S1 for the PDDG and AM1 hybrid potentials, respectively. Overall we consider this mechanism unlikely for the reasons given below.

Construction or minimization of NEB pathways between the G and A1 states failed or gave unreasonably high energy barriers (not shown). The occurrence of an ESPT from Tyr63 to His62 in this step was anticipated from the known strong decrease of the hydroxybenzylidene pK_a in S_1.[33] In avGFP, the proton is transferred to Glu222 (corresponding to Glu212 in EosFP) via a hydrogen-bonding network.[34] Such a network between Tyr63 and His62 does not appear to exist in EosFP, based on the crystallographic structures in ground state S_0, and it is difficult to identify a realistic path that could transiently form in S_1, given the essentially identical geometry of our excited-state model and the ~11 Å distance that separates the hydroxyl group of Tyr63 and the N_ε atom of His62 (Figure 1b). Moreover, the N_ε atom of His62 resides in a nonpolar environment unfavorable for protonation.

The next step in the mechanism of Scheme 1 is the cleavage of the $C_\alpha-N$ bond from the imidazolium-based A1 state. This step appears unlikely to occur as it requires crossing an energy barrier approaching 150 kJ/mol. It is followed by an intraresidue proton transfer within Phe61 (A2 to A3) and by the second step of the β-elimination reaction, which involves proton transfer from C_β of His62 to the carboxylate group of Glu212 (A3 to A4). Together, these steps have small energy barriers and result in a large decrease in energy. By contrast, the last step (A4 to RA) again requires crossing a substantial energy barrier of ~75 kJ/mol. This step involves proton transfer from N_ε to N_δ of the imidazole via an intermediate characterized by a sp3-hybridized C_ε. This rearrangement is necessary to restore the hydrogen bond between the carbonyl moiety of Phe61 and the N_δ atom of His62.

A New Proposal. The previously discussed mechanism starts with an ESPT from the hydroxybenzylidene moiety of the chromophore. As an alternative, we propose that the chromophore remains protonated during the entire photoconversion process and that backbone cleavage is a direct consequence of excitation of the neutral chromophore. To investigate this hypothesis, we tested the mechanism shown in Scheme 2, in which Glu212 acts as the proton acceptor in the β-elimination. We started off by optimizing NEB pathways between the G and B4 species on the first singlet excited state (S_1) surface. The resulting energy profiles are shown in Figures 3a and S2a.

The first event along the optimized NEB path is an ESPT from the N_δ atom of His62 to the carbonyl moiety of Phe61. The energy of this proton transfer was determined to be ~25 kJ/mol with the PDDG potential. To our knowledge, an ESPT from the N_δ atom of a neutral imidazole ring has not been reported. However, a fluorophore with an imidazolide ring was

(33) Chattoraj, M.; King, B. A.; Bublitz, G. U.; Boxer, S. G. *Proc. Natl. Acad. Sci. U.S.A.* **1996**, *93*, 8362–8367.
(34) Brejc, K.; Sixma, T. K.; Kitts, P. A.; Kain, S. R.; Tsien, R. Y.; Ormo, M.; Remington, S. J. *Proc. Natl. Acad. Sci. U.S.A.* **1997**, *94*, 2306–2311.

Scheme 2. Suggested Photoconversion Mechanism with Glu212 as Proton Acceptor (B4) and Intermediate Structures Derived from Simulation[a]

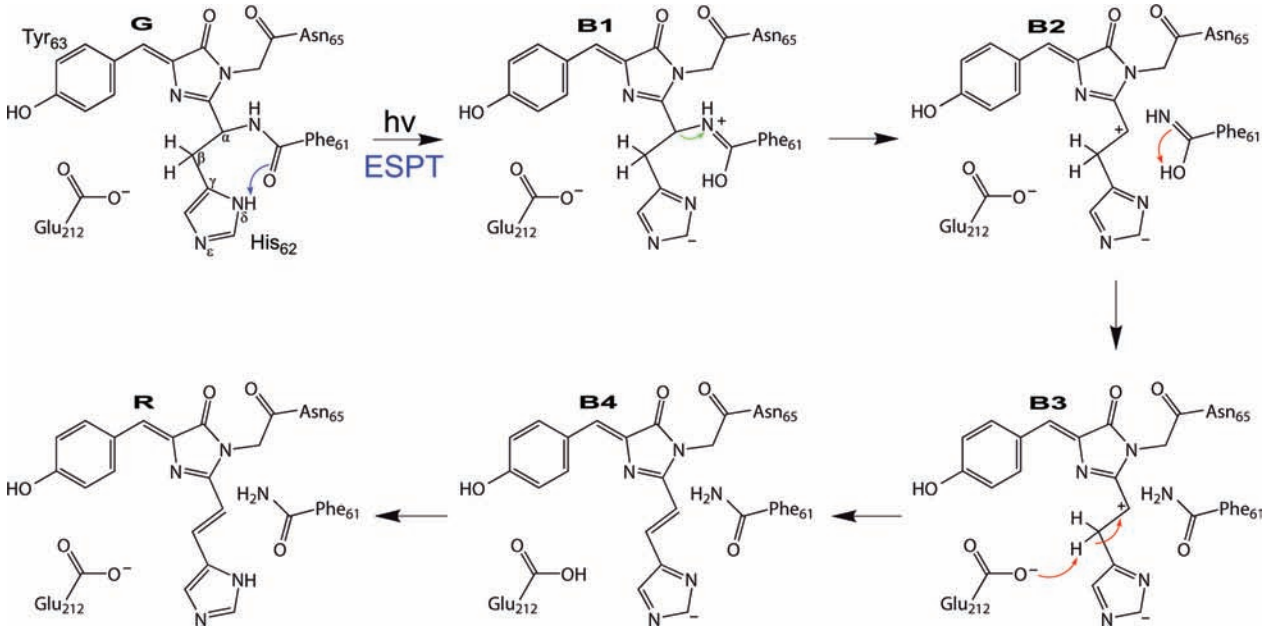

[a] Arrows show the main reaction steps in the color of the electronic state involved: blue for S_1, green for T_1, red for S_0.

recently found under basic conditions,[35] indicating that the usual pK_a of the imidazole ring can be significantly lowered in the presence of certain functionalities. In EosFP, the stereochemical alignment between the N_δ atom of His62 and the carbonyl moiety of Phe61 probably favors ESPT, which may be further facilitated by tunneling effects.[36,37] The occurrence of an ESPT involving an imidazole ring also likely accounts for the fact that His62 is strictly conserved in all PCFPs.

On the S_1 excited state surface, the activation energies for breaking the $C_\alpha-N$ bond is ~110 kJ/mol. This barrier is too high to be crossed, considering the short lifetime of the S_1 state, which is estimated to be of the order of a nanosecond. However, at the B1 intermediate, a conical intersection between the S1 and first excited state triplet (T1) surfaces appears. This conical intersection suggests that, to reach B4 from G, there must be an intersystem crossing from the S_1 to T_1 surfaces, which we denote ISC1 (Figures 3a and S2a).

Making this assumption, we reoptimized NEB pathways for the transition between the B1 and B4 structures of Scheme 2 on the T_1 surface (Figure 3b and S2b). At the B1 intermediate, a positive charge is localized on the nitrogen of the $C_\alpha-N$ bond. As a result, only ~15 kJ/mol are required to activate the $C_\alpha-N$ bond cleavage. At B2, the T_1 and S_0 surfaces become degenerate and remain so until formation of the B3 intermediate, after which the ground state S_0 becomes lower in energy. This suggests a second intersystem crossing, ISC2, occurring between the B2 and B3 intermediates.

We calculated also the minimum energy paths between G and B4 intermediates on the S_0 and T_1 surfaces (Figure S3). In contrast to what was observed for the S_1-optimized pathways (Figures 3a and S2a), cleavage of the $C_\alpha-N$ bond is accompanied by proton transfer from the N_δ atom of His62. Thus, neither a separate B1 intermediate nor an associated conical intersection are observed. To reach B2 from G, activation energies are very high, being ~135 and ~300 kJ/mol on the S_0 and T_1 surfaces, respectively. This implies $C_\alpha-N$ bond cleavage is unlikely in the S_0 and T_1 states, which is supported, at least for the ground state S_0, by the inability of PCFPs to convert in the dark.

Role of Glu212 in the Photoconversion. Glu212 is known to be essential for photoconversion of EosFP, as mutation of this residue to a glutamine (E212Q) abolishes the reaction.[4,17] Nienhaus et al. therefore suggested that the glutamate may act as a proton acceptor,[4] whereas Mizuno et al. proposed that it participates in the stabilization of the transition state.[6]

In our Scheme 2 that implicates Glu212 as a proton acceptor, we found that the proton transfer from C_β of His62 to the Glu212 carboxylate occurs between intermediates B3 and B4 on the S_0 surface (Figures 3b and S2b). To investigate the back proton transfer from Glu212 to the N_δ atom of His62, we optimized NEB pathways on the S_0 surface starting from B4 and going to the final red structure R. The optimized profiles are shown in Figures 3c and S2c. Overall the process is complex and involves a return of the proton to the C_β atom of His62 in a B3-like state, in which the S_0 and T_1 states are degenerate, and with an activation barrier of ~55 kJ/mol. This suggests that B4 may not be involved in the actual photoconversion pathway.

To check if another mechanism is possible that does not involve protonation of Glu212, we optimized NEB pathways from the second intersystem crossing ISC2 to the final red structure on the ground state surface S_0. The full mechanistic pathway is shown in Scheme 3, and the optimized NEB profiles in Figures 4 and S4.

First of all, the B2 intermediate has a carbocation on the C_α atom of His62. This makes the C_β atom very acidic, and delocalized electrons on the imidazolide make the C_γ atom a strong base, much more so than the carboxylate of Glu212. Therefore, in the step from B2 to C3, the proton on C_β is spontaneously transferred to the C_γ of the imidazolide moiety

(35) Berezin, M. Y.; Kao, J.; Achilefu, S. *Chemistry* **2009**, *15*, 3560–3566.
(36) Stoner-Ma, D.; Jaye, A. A.; Ronayne, K. L.; Nappa, J.; Meech, S. R.; Tonge, P. J. *J. Am. Chem. Soc.* **2008**, *130*, 1227–1235.
(37) Violot, S.; Carpentier, P.; Blanchoin, L.; Bourgeois, D. *J. Am. Chem. Soc.* **2009**, *131*, 10356–10357.

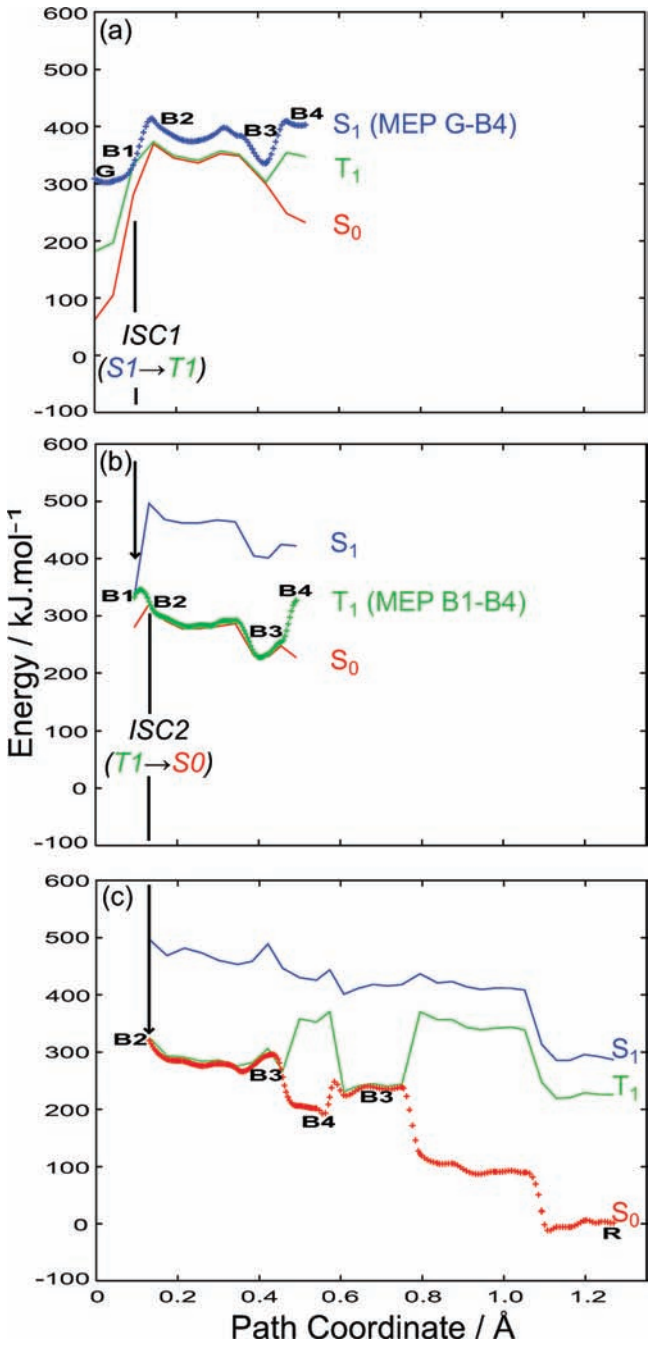

Figure 3. Energy profiles of optimized NEB paths calculated with a [10,9]-CISD(PDDG)/OPLS hybrid potential: (a) from G to B4 in the excited state S_1 (blue plus signs), (b) from B1 to B4 in the excited state T_1 (green plus signs), and (c) from B2 to B4 and from B4 to R in the ground state S_0 (red plus signs). Solid lines in each panel represent the energies of the optimized NEB structures in the electronic states that were not used in the optimization.

and a double bond is formed between C_α and C_β. The same proton is then transferred to the N_δ of His62, and the imidazole ring is reformed. In the last step, the proton on the Phe61 carbonyl rearranges to form the carboxamide. Overall, the complete process is energetically downhill, and the highest energy barrier for any of the proton transfers is ~25 kJ/mol.

KikGR Specificities in the PCFP Family. In the PCFP family, KikGR differs from the other members in that the His62 side chain isomerizes along the photoconversion pathway. The mechanism depicted in Scheme 3 accounts for this specificity. We propose that isomerization of the His62 side chain occurs in the B2 intermediate state, by rotation about the $C_\alpha-C_\beta$ single bond, taking advantage of the long lifetime of the triplet state before ISC2 takes place. After rotation, formation of the double bond follows and the final proton transfers lead to the red (isomerized) state. In EosFP and Kaede, residue Ile196 in the vicinity of His62 is engaged in hydrophobic interactions with Leu210 and does not leave enough space for isomerization of the His62 side chain (Figure 5a). The situation is different in KikGR, in which Ile196 and Met40 of EosFP are swapped to Met198 and Val40. As a result, Leu212 maintains a hydrophobic interaction with Val40 and leaves Met198 free of interaction. This provides conformational freedom to Met198, which allows His62 isomerization to occur (Figure 5b).

Another specificity of KikGR in the PCFP family is the absence of water molecule W1 in the green form (Figure 5b). For Kaede and EosFP, Hayashi et al. proposed that W1, which disappears in the red form of these proteins (Figure 5a), may assist in photoconversion.[6] In our study, we were unable to find evidence for such involvement of W1. The absence of the water molecule in the crystal structure of KikGR also suggests that it is not essential for the reaction. In our models of green EosFP, W1 is hydrogen-bonded to the side chain oxygen atom of Gln38, to the carbonyl group of Ser39 and, to a lesser extent, to the C_ε atom of His62. The latter two interactions are disrupted during our simulations of photoconversion, and formation of the imidazolide moiety on His62 induces their replacement by hydrogen bonds to the side chains of two neighboring residues (Met40 and Ile10). In our models of red EosFP, because our methods require keeping the same number of atoms throughout the simulations, the hydrogen bonds observed in the green form are restored. We suggest that, in the real mechanism, rearrangements that occur during photoconversion induce transient weakening of the interactions maintained by W1, which leads to the exit of this water molecule from the protein.

Electronic Structure of Intermediates. Figure 6 is a schematic that illustrates the electronic structures of the various intermediates along the photoconversion pathway of Scheme 3 obtained with the PDDG potential. For each intermediate, cartoons of the most important electronic configurations in each electronic state are given, together with images of the orbitals that are involved.

Overall, the majority of the intermediates' electronic states are dominated by a single electronic configuration of the appropriate type. The G electronic states are of simple type except that excitation involves the HOMO-1 rather than the HOMO. As these orbitals are localized on the hydroxybenzylidene-imidazolinone and the His62 imidazole moieties, respectively, the S_1 and T_1 states retain charge density on His62. By contrast, for the B1 intermediate, the excitation to S_1 and T_1 comes from the HOMO even though this orbital and the LUMO have character very similar to those of G. Thus, there is charge transfer between the His62 imidazolide moiety (where the HOMO is localized) and the hydroxybenzylidene-imidazolinone group (where the LUMO is localized), which explains why the S_1 and T_1 states are degenerate, as the two unpaired electrons in the HOMO and the LUMO are in different regions of space and interact only weakly.

At the B2 intermediate, T_1 retains its simple form, although the orbitals involved, the HOMO and LUMO, have electron density concentrated on the imidazolide and imidazolinone moieties but little on the phenol group. S_0 and S_1 are more complicated. S_1 has no compact description, whereas S_0 has

Scheme 3. Photoconversion Mechanism with the Intermediate States (C3, C4) Derived from Simulation[a]

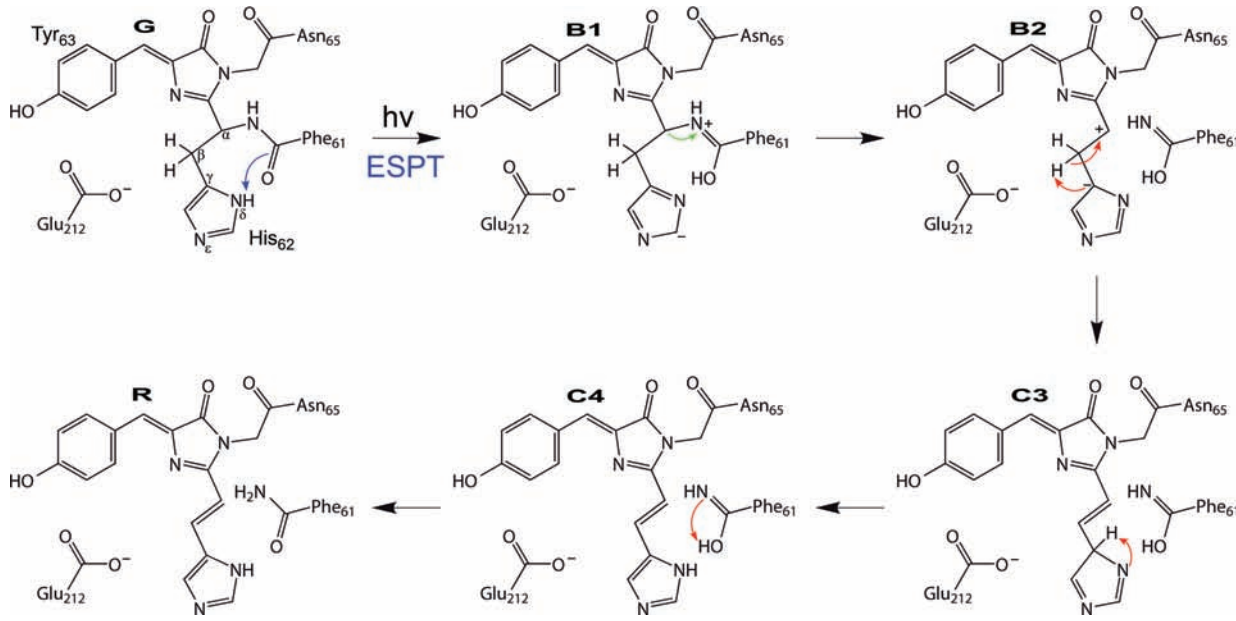

[a] Arrows show the main reaction steps in the color of the electronic state involved: blue for S_1, green for T_1, red for S_0.

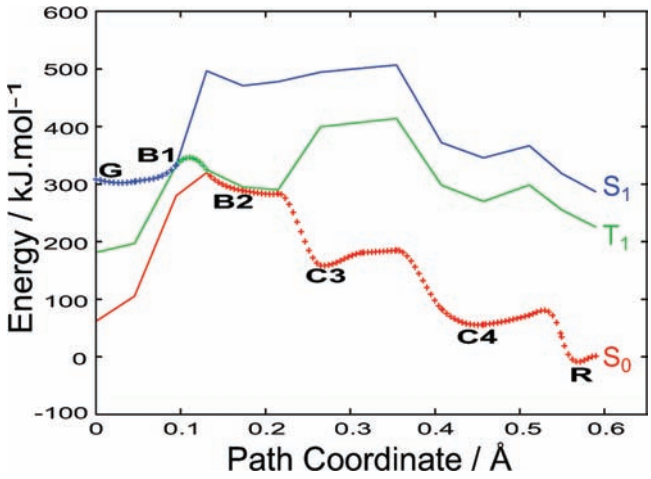

Figure 4. Energy profile of optimized NEB paths calculated with a [10,9]-CISD(PDDG)/OPLS hybrid potential from G to B1 in the excited state S_1 (blue plus signs), from B1 to B2 in the excited state T_1 (green plus signs), and from B2 to R in the ground state S_0 (red plus signs). The solid lines represent the energies of the optimized NEB structures in electronic states that were not used during optimization.

significant contributions from the two closed-shell configurations that are possible by doubly occupying the HOMO and LUMO. These are the same orbitals that are singly occupied in T_1 and indicate why the S_0 and T_1 states are degenerate for this intermediate.

After B2, the mechanism continues on the S_0 surface. The remaining electronic states are all of simple type, except for the S_1 and T_1 states of the red form R, which involve a mixture of two configurations obtained by excitation from the HOMO-1 and the HOMO, respectively.

Anionic Form of PCFPs. Activation with cyan light (~488 nm) of the anionic form of EosFP chromophores does not induce significant photoconversion. To better understand the role of the protonation state, we calculated first the NEB pathways between anionic forms of G and B4 intermediates on the S_1 surface (Scheme 2). The $C_\alpha-N$ bond cleavage is accompanied by proton transfer from the N_δ atom of His62, and the activation energy is very high at ~170 kJ/mol (Figure 7a and S5a). This finding is in agreement with the impossibility of photoconverting anionic forms of EosFP.

As a second test, we recalculated the energy profiles of photoconversion that were obtained for the neutral forms after removing the proton on the chromophore of each structure. The profiles are shown in Figures 7b and S5b. Clearly, the presence of the extra negative charge on the chromophore is likely to stabilize the starting S_1 state of G due to electrostatic interactions between Tyr63 and the cationic His194, while perhaps destabilizing the S_1 state of B1 because formation of the negatively charged imidazolide is less favorable. These trends rationalize why the NEB pathways optimized for cleavage with an anionic chromophore do not go through a B1-like structure, because the putative activation barrier in S_1, approaching 200 kJ/mol (Figures 7b), is larger than for the concerted reaction (Figures 7a).

Even if anionic forms of EosFP underwent the initial ESPT between His62 and Phe61, the expected ISC1 event could not occur since the conical intersection disappears for the B1 structure (Figures 7b). Indeed, T_1 and S_1 excited states of this intermediate are not degenerate since their electronic structure is now markedly different (Figure S6). Overall, these results show the obstacles that exist for a photoconversion pathway involving an anionic chromophore in PCFPs.

Catalytic Effects inside PCFPs. The three-dimensional structure of PCFPs plays a crucial role in the photoconversion mechanism, since denaturated forms of green species cannot be cleaved under UV irradiation.[12] This influence of the protein matrix on the reaction mechanism was investigated by recalculating the energies of the structures along the optimized pathways in vacuo, i.e., by excluding all MM atoms and the side chains of His194 and Glu212. The results are shown in Figures 8a and S7a and indicate a clear stabilization of the S_1 and T_1 (degenerate) states of the B1 intermediate by the protein. The energy difference between the G and B1 species in the S_1 state, which presumably constitutes the most critical activation

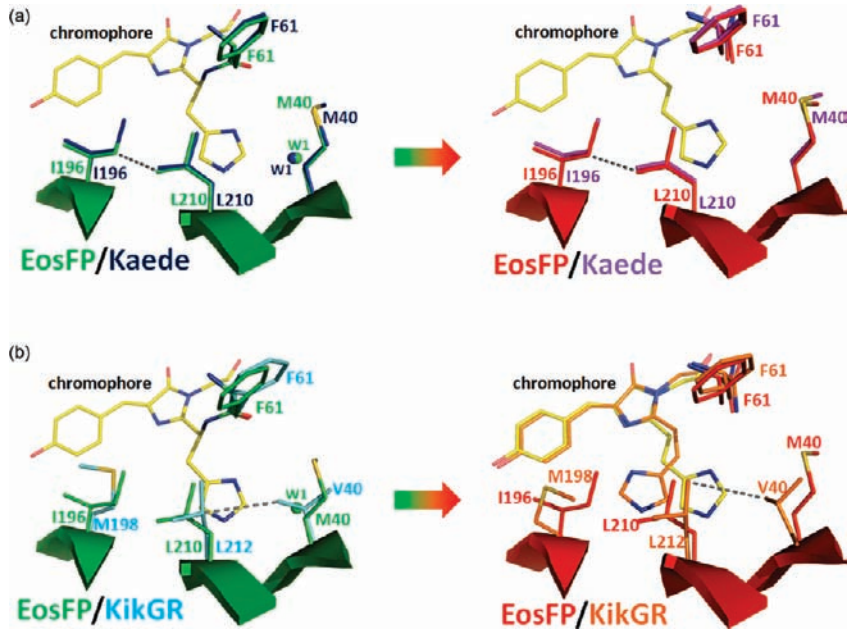

Figure 5. Superposition of structures of EosFP with (a) Kaede and (b) KikGR in the chromophore region before (left) and after (right) photoconversion (hydrophobic interactions are indicated by dashed lines).

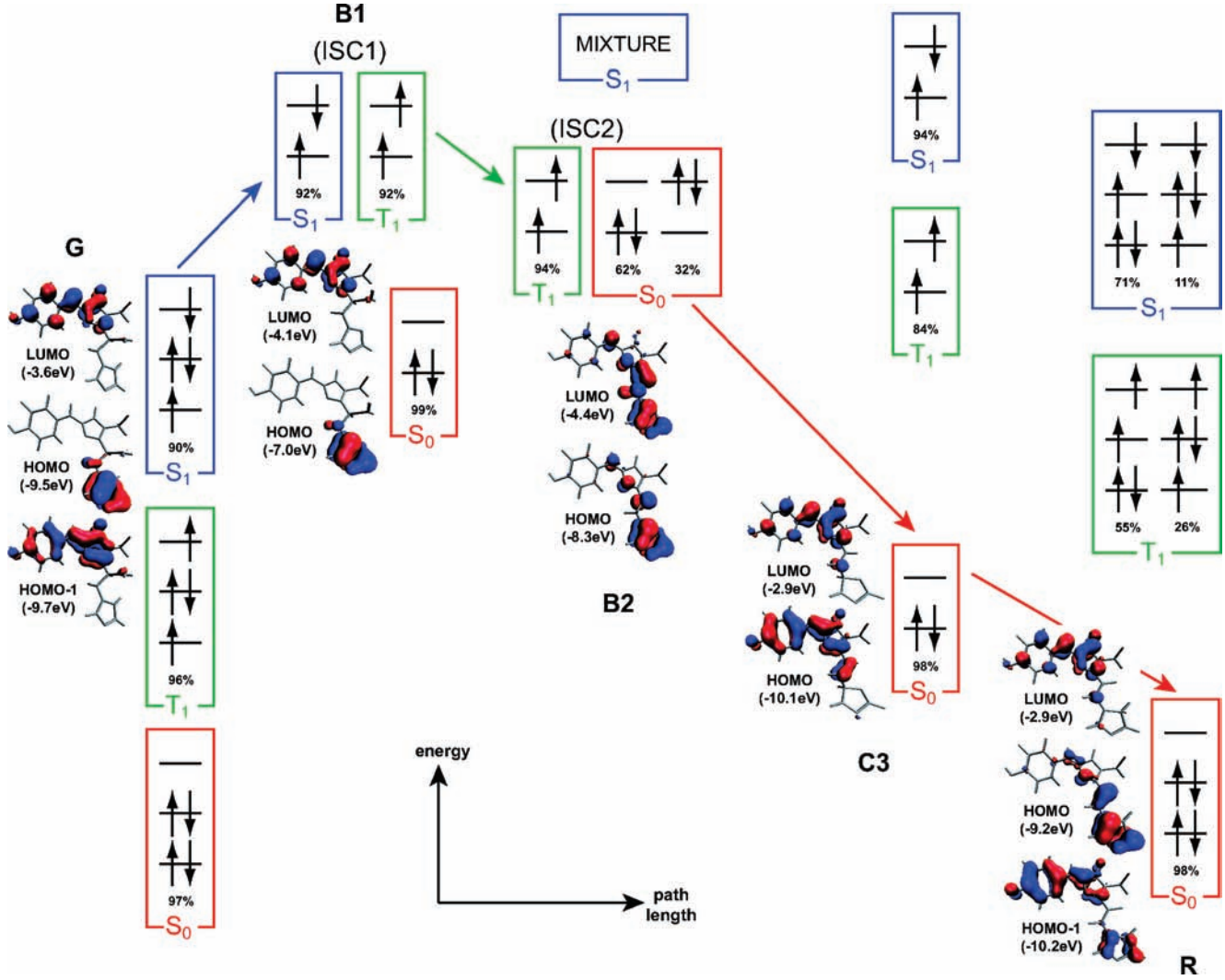

Figure 6. Schematic of the electronic states along the photoconversion path calculated with a [10,9]-CISD(PDDG)/OPLS hybrid potential. For convenience, triplet configurations are represented by a single microstate (S = 1; Sz = +1), as are singlet configurations with two unpaired electrons (electrons with opposing spins in two different orbitals). The fractional weights of the states, however, include contributions from all equivalent configurations. For each structure, only molecular orbitals involved in the excitation are shown.

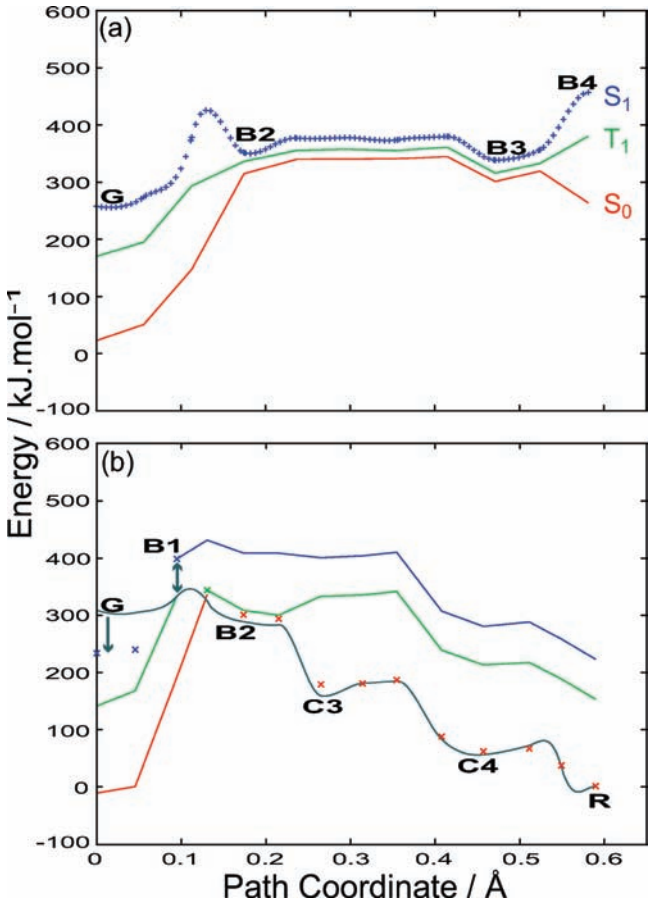

Figure 7. (a) Energy profile of optimized NEB path calculated with a [10,9]-CISD(PDDG)/OPLS hybrid potential between anionic forms of G and B4 in the excited state S_1 (blue plus signs). The solid lines represent the energies of the optimized NEB structures in electronic states that were not used during optimization. (b) Energy profile of the photoconversion pathway obtained with a [10,9]-CISD(PDDG)/OPLS hybrid potential for the neutral structures in which the proton has been removed from the phenol ring of the chromophore. Energies of the resulting anionic structures are calculated in the S_0 (red), T_1 (green), and S_1 (blue) electronic states. Crosses show the energy points along the reaction path; the main deviations to the neutral form profiles (shown in gray) are indicated by arrows. The solid lines represent the energies of the structures in the other electronic states.

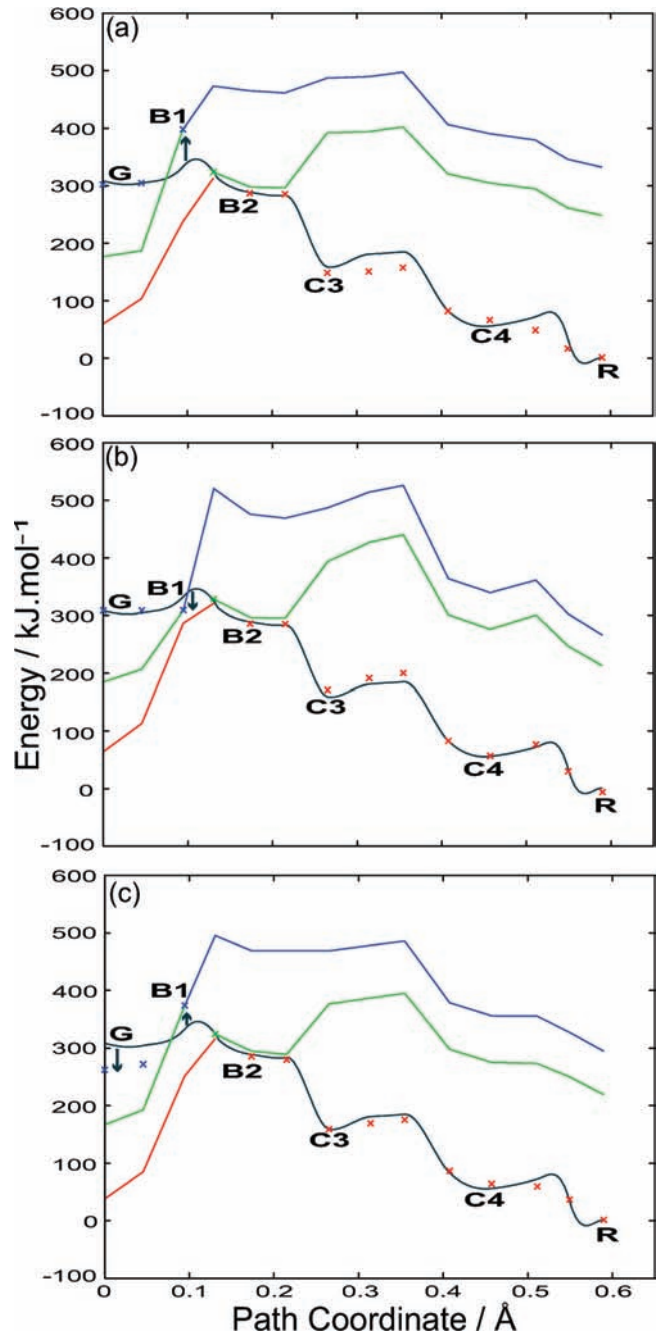

Figure 8. Energy profile of photoconversion calculated: (a) for the chromophore in vacuo with a [10,9]-CISD(PDDG) potential, (b) in protein with null atomic charges (MM) on Glu212, and (c) on His194, with a [10,9]-CISD(PDDG)/OPLS hybrid potential for which His194 and Glu212 are located in the MM region. Energies of structures extracted from the original NEB path (neutral chromophore in protein with the initial QC/MM partitioning) are calculated with the modified potentials in the S_0 (red), T_1 (green), and S_1 (blue) electronic states. Crosses show the energy points along the reaction path; the main deviations to the original profile (shown in gray) are indicated by arrows. The solid lines represent the energies of the structures in the other electronic states.

barrier to be crossed due to the short lifetime of the excited state, is shifted from ~25 kJ/mol in the protein to ~95 kJ/mol in vacuum.

To more fully understand this catalytic effect, the energies of the structures along the optimized NEB pathways were recalculated with a new QC/MM partitioning in which Glu212 and His194 were excluded from the QC region. The profiles, which are shown in Figure S8, are indistinguishable when superimposed on the optimized ones, suggesting that the role of these residues can equally well be described with a ground-state MM potential. In the same way, the energy profiles in vacuo were recalculated with two different TDDFT methods, in order to check the reliability of our excited state potentials. The profiles, which are shown in Figure S9, are qualitatively similar to those obtained with the semiempirical CI methods.

To probe the specific effects of various residues on the photoconversion mechanism, the profile calculations were repeated by systematically setting the MM charges on each residue within the mobile region to zero. This change has minimal effect on the profiles except for Glu212 and the three positively charged residues, His194, Arg66, and Arg91, which are found closest to the hydroxybenzylidene-imidazolinone moiety (Figure 1b).

The profiles with no MM charges on Glu212 are displayed in Figures 8b and S7b. They indicate that removal of the residue's negative charge actually stabilizes the S_1 and T_1 excited states of B1 and has little effect on the remainder of the pathway.

This result is at variance with the suggestion of Hayashi et al. for rationalizing the key role of this residue.[6] The profiles for His194 are shown in Figures 8c and S7c. Both display a stabilization of the green form (structure G) and a destabilization of the B1 intermediate on the S_1 surface. Further analysis shows mainly that the electronic structure of the B1 intermediate is similar to the one of Figure 6 (see Figure S10), although the absence of the positive charge on His194 destabilizes the LUMO that is localized on the hydroxybenzylidene-imidazolinone group, from −4.1 to −3.1 eV (or ∼95 kJ/mol), thereby leading to higher energies for S_1 and T_1 (Figures 8c). Consequently, the energy difference between the G and B1 structures in the S_1 state increases from ∼25 to ∼110 kJ/mol, equivalent to a factor of ∼4.5. When compared to His194, the two arginines, Arg66 and Arg91, show similar, but less pronounced, catalytic effects on the photoconversion energy profiles (Figure S11). Clearly, these three positively charged residues, and particularly His194, might have a crucial stabilizing effect on the transition state leading to backbone cleavage.

The results discussed above can also account for the fact that the E212Q variant of EosFP does not undergo photoconversion, even though, according to our results, Glu212 itself does not participate in the reaction. Glu212 hydrogen bonds directly to His194 and indirectly, via a water molecule (W3 in Figure 1b), to Arg66. Hence, it is possible that in the E212Q mutant, His194 can no longer be biprotonated or that, due to the disruption of the hydrogen-bond network around the chromophore, the critical Arg66 residue is displaced, thus impeding photoconversion. This possibility is substantiated by the observation that the E212Q mutation increases the pK_a of Tyr63 by 0.8 unit (6.6 vs 5.8 in wtEosFP), suggesting important modifications in the hydroxybenzylidene-imidazolinone environment.[17] The crucial role of Arg66 in shifting the Tyr63 pK_a found in Dendra2[15] also agrees with this hypothesis. Similar indirect effects could account for the loss of activity reported in other PCFP mutants, such as the A69S variant of Kaede.[12]

Optimization Strategies for PCFPs. Based on our findings, one may speculate that the introduction of additional positively charged residues in the chromophore environment, or of mutations that result in an improved network of positive charges, could facilitate photoconversion. However, whereas lowering the hydroxybenzylidene pK_a, as observed in Dendra2, effectively achieves this goal by increasing the fraction of protonated chromophores at physiological pH,[15] it is expected that the yield of photoconversion cannot be improved to an appreciable extent. In the mechanism proposed in Scheme 3, photoconversion is inherently limited by the two intersystem crossings that lead to transitions between potential energy surfaces.

Overall, we assign the slow kinetics that is experimentally observed in PCFPs to the requirement for two low-yield intersystem crossings events. This also accounts for the somewhat surprising finding that such a low yield process is accompanied by only very small structural changes between the green and red states in PCFPs.

Conclusion

We have investigated the mechanism of photoconversion between the green and red forms of the fluorescent protein EosFP using hybrid QC/MM potentials in conjunction with reaction-path-finding techniques. The preferred pathway identified from our simulations involves excitation of the green protonated form to the S_1 state, followed by two intersystem crossings (ISCs), first to the T_1 state and then to the S_0 ground state. Proton transfer from His62 to the carbonyl group of Phe61 occurs on the S_1 surface, forming an imidazolide ring on His62 side chain. Cleavage of the amide bond between Phe61 and His62 then becomes possible on the T_1 surface. Completion of the red form occurs on the S_0 surface via a series of proton transfers that are downhill in energy, extend the π-conjugated system, and lead to the reformation of the imidazole ring on the His62 side chain.

The occurrence of ISCs is a novel aspect of the photoconversion mechanism in PCFPs and provides an explanation for the observed low quantum yield of the process. The mechanism proposed in this work differs from previous hypotheses in a number of ways: (i) The phenol ring of the chromophore does not undergo an ESPT and remains protonated along the whole reaction pathway. (ii) The essential residue Glu212 remains deprotonated throughout and does not take part in proton transfer. (iii) Water molecules in the vicinity of the chromophore are not involved. An analysis of the structures and energetics of the intermediates along the pathway shows that three cationic residues closest to the chromophore have important catalytic roles, whereas Glu212, which is itself anticatalytic, indirectly serves to maintain the integrity of the chromophore's electrostatic environment. These results suggest that engineering EosFP by reorganizing or introducing extra cationic residues around the chromophore could facilitate photoconversion.

Acknowledgment. We thank Antoine Royant for fruitful discussions. We also thank the Ministère de l'Enseignement Supérieur et de la Recherche, the Centre National de la Recherche Scientifique, the European Synchrotron Radiation Facility, and the Agence Nationale de la Recherche (ANR-07-BLAN-0107-01) for financial support. This work was further supported by the Deutsche Forschungsgemeinschaft (DFG) and the State of Baden-Württemberg through the Center for Functional Nanostructures (CFN) and by DFG grants NI 291/9 and SFB 497.

Supporting Information Available: Table of absorption and emission wavelength predicted by the QC/MM potentials used in this work, additional figures, and comments on alternative reaction pathways. This material is available free of charge via the Internet at http://pubs.acs.org.

JA905380Y